Automatic Measurement of Fish Weight and Size by Processing Underwater Hatchery Images

Sanchez-Torres G., Ceballos-Arroyo A., and Robles-Serrano S.

***Abstract*— Retrieving information from fish hatcheries is a key need in the Colombian fishing industry because it allows hatchery managers to determine necessary food amounts and measure other population parameters. However, traditional measurement methods involve extracting live fish from the ponds. This results in stress and the possibility of injury. Researchers have proposed automated measuring systems for shortening measurement times and reducing fish stress, but they must fulfill several prerequisites before they can retrieve fish information. These include mounting underwater camera systems and applying image enhancement and segmentation algorithms. In this paper, the literature revolving around these issues is reviewed and a novel approach is proposed. It is shown that using a single camera for image acquisition in a controlled setup is appropriate because it enables better management of sample size and image acquisition conditions. Furthermore, a combination of homomorphic filtering, contrast limited adaptive histogram equalization (CLAHE) and guided filtering for fish image enhancement was used. The fish were then segmented using a combination of 2D saliency detection and morphological operators. Finally, fish length was obtained using a third-degree polynomial regression on the fish mid-points. The length was calculated to estimate the weight with several regression algorithms. This approach was shown to be the most appropriate method for regression of fish weight based on length**.

***Index Terms*— Image processing, underwater images, image segmentation, algorithms, saliency, contrast, fishes.**

I. Introduction

THE Colombian fishing industry is a well-established sector whose economic relevance increases as demand grows [1]. In response, government entities have put forward several policies for modernizing the sector and incentivizing its development [2][3]. In the context of fish production research, one basic activity is collecting and processing data from individuals for estimating population information [4][5]. Usage of this information is extensive because it allows administrators to determine required food amounts for the hatcheries, automate the sorting and classification of fish to catch, guarantee commercialization of required fish species and sizes [6] and develop strategies for management and preservation of species [7].

Aquiculture researchers have made significant progress regarding measurement techniques and associated instrumentation for efficiently gathering data [8]. However, physical contact with the fish limits traditional methods because invasive techniques can cause lesions or increase stress levels. The development of technologies for collecting fish data without human intervention is the key for technological research and engineering applications [9]. Although there is published work in which authors carried out these measurements using digital image processing-based systems, the software tools for this purpose are not widely available and they are challenging to adapt to local conditions.

As a response, this work proposes a pipeline for the acquisition, enhancement and automatic segmentation of fish using underwater images in order to estimate length and weight.

II. Methodology

The proposed acquisition system, image pre-processing pipeline, fish segmentation algorithm and the method for estimating fish properties are described in this section. Figure 1 summarizes this process.

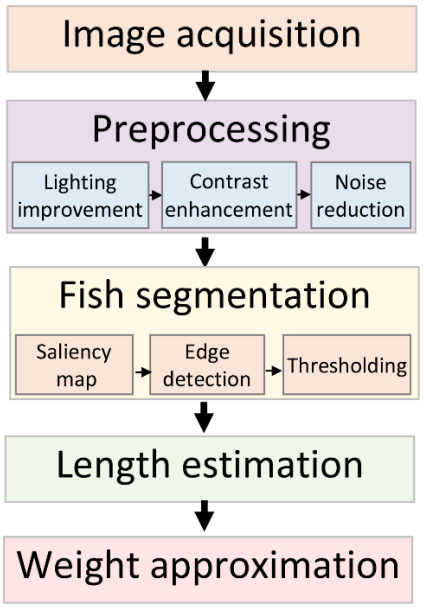

Fig. 1. Outline of the procedures employed to segment fish.

A. Image Acquisition

Although the main goal of many research projects is to automate fish counting and measurement, it is necessary to

Manuscript received April 24, 2018. This work was supported by the Universidad del Magdalena in the context of the research project Estimación automática del peso y longitud de peces mediante técnicas de visión por computador.

Sanchez-Torres G., Ceballos-Arroyo A., and Robles-Serrano S., are with the Faculty of Engineering, Universidad del Magdalena, Carrera 32 No. 22-08, Santa Marta, Colombia. (e-mail: gsanchez@unimagdalena.edu.co, albertoceballosma@miunimagdalena.edu.co, sergioroblesas@miunimagdalena.edu.co).

first design an appropriate image acquisition system. This choice defines the algorithms that are implemented to extract fish information. The literature describes several methodologies for obtaining fish images, and they can be sorted into two categories: single image and multiple image systems.

Single image systems take and process only one input image. They require the distance between the fish and the lens to be known or estimable. Hardin [10] used a monochromatic 30 FPS progressive scan Hitachi KP-F2A camera to ensure the lateral view of the fish was captured entirely in at least one frame. Once calibrated, the camera captured images at a constant rate until fish detection. Two lights placed on both sides of the camera and a white background opposite to it maximized the amount of light in the scene.

Multiple image systems are based on taking two or more images using stereo vision techniques. In stereo-vision systems, the cameras capture several images at the same time from different angles. This results in increased processing cost but enables depth perception [26]. In stereo-vision systems, a known distance in a single axis separates the cameras and the measurement algorithm uses said distance as a parameter. This kind of technique does not require the fish to be at a fixed position, distance or orientation concerning the cameras.

For this work, the single image-based methods were selected because they are computationally simpler. High-contrast backgrounds and backlighting were used to improve and simplify the fish segmentation without losing measurement precision.

Table 1 shows some of the most relevant examples of systems for capturing images of fishes in underwater environments.

TABLE 1. A LITERATURE REVIEW OF UNDERWATER IMAGE CAPTURE SYSTEMS.

Author	Environment	C	Features
(Strachan *et al.*, 1993)	Conveyor belt.	1	+ The system makes fish segmentation easier. - The methodology is not adequate for live fish segmentation.
(Petrell *et al.*, 1997)	Free environment (pond).	2	+ Authors achieve similar precision to that of many manual methods.
(Tillett *et al*., 2000)	Free environment (pond).	2	+ Precise stereo image-based estimation of fish proportions. - The authors do not consider adequate sampling methods.
(Lines *et al.*, 2001)	Free environment (pond).	2	+The authors estimate fish properties using stereo photography. -The authors do not propose a methodology for simplifying underwater segmentation.
(Chambah *et al.*, 2003)	Free environment (aquarium).	1	+The system allows segmentation and classification of fishes from different species in an open environment. -The users need to manually focus the camera. -There is no fish measurement to speak of.
(Martinez-De Dios *et al.*, 2003)	Free environment (pond).	2	+Authors measure fishes without using invasive methods. +The method makes segmentation easier when fishes overlap. -The authors do not address the issue of sample bias.
(Lee *et al.*, 2004)	Controlled environment (hydroelectric dam waterways).	1	+The authors extract fish borders using a single camera. -Classification accuracy is weak and the authors do not measure the fishes.
(Hardin, 2006)	Controlled environment (hydroelectric dam waterways).	1	+The author uses several materials for modifying the environment and making it closer to ideal conditions. +The author exploits environment stability for making segmentation tasks easier. -The methodology is highly specific to the studied species and setting.
(White *et al.*, 2006)	Conveyor belt.	1	+The setup simplifies fish segmentation. -The methodology is not adequate for live fish segmentation.
(Costa *et al.*, 2006)	Free environment (pond).	2	+Authors carry out fish measurements without the need to construct a tunnel. -The system has limited measurement accuracy.
(Lam *et al.*, 2007)	Free environment (open sea reef).	1	+The system enables tracking and classification of fishes in an uncontrolled environment. -There is no fish measurement to speak of.
(Zion *et al.*, 2007)	Controlled environment (single camera in pond).	1	+The authors deploy an efficient, high quality and non-invasive system.
(Costa *et al.*, 2013)	Fixed surface.	1	+High accuracy in anomaly measurement and classification. -The authors do not contemplate measuring live fish.
(Liu *et al.*, *2016*)	Conveyor belt.	1	+The setup makes segmentation easier due to the contrast between the individuals and the surface. -Authors do not measure objects of interest.
(Qin *et al.*, 2016)	Free environment (open sea).	1	+The system captures videos of fishes in schools in an open sea environment. -The authors do not measure fish size.
(Miranda *et al.*, 2017)	Controlled environment (single camera system in the pond).	1	+The authors propose an automatic and non-invasive measurement technique. + The system makes fish measurement easier. -The setup is highly specific to the studied species.

C: number of cameras the authors use.
+ Positive aspects.
- Weak aspects.

B. Image pre-processing

Several difficulties arise when processing underwater images (UI) and depend on the depth of the water [27]. A medium density, turbidity and refraction result in low visibility. A limited contrast, the prevalence of specific colour tonalities and a restricted visibility range of 5 to 20 meters also result [28] [29]. Due to this, the physical phenomena caused by the environment and noise caused by inorganic and organic matter were considered when processing the underwater images [30].

The UI treatment techniques are a pre-processing tool for computer vision applications requiring object identification in underwater environments [16]. The UI treatment methods can be classified into two categories, namely restoration and enhancement techniques [28]. The former defines a degradation simulation model for reconstructing the original image and the latter attempts to improve visibility by manipulating image components. Enhancement is usually faster and more straightforward than restoration because it does not involve physical models or image generation. The UI enhancement provides an improved image as the output when a low-quality image is given as the input [31]. Such techniques usually improve image quality by enhancing the contrast and reducing noise [28] [32].

The UI enhancement techniques in this work were classified based on their approach [28], as histogram and contrast manipulation, Retinex model based, filter based and polarization or stereo photography methods. These categories are not mutually exclusive because mixed methodologies exist that combine several algorithms, and individual algorithms may belong to more than one category [28]. Furthermore, some techniques are unique enough to not fit within any of the previously mentioned classes. A taxonomy of the work centred on UI enhancement consists of four main categories:

- Histogram, contrast stretching and manipulation-based techniques.
- Retinex model-based techniques.
- Filter based techniques
- Mixed techniques.

A set of procedures was selected to handle the three main issues in UI enhancement and obtain the most appropriate sequence for subsequent fish identification. These three issues include unbalanced lighting, limited contrast and noise presence. Based on the analysis reported in [30], recurring procedures in the literature include homomorphic filtering and contrast limited adaptive histogram equalization (CLAHE). Additionally, guided filtering was used instead of bilateral filtering due to its reduced computational cost, noise removal and border preserving capabilities. Figure 2 shows the proposed sequence.

Fig. 2. Modified version of the sequence proposed in [30].

The homomorphic filter is a nonlinear filter that is able to transform multiplicative features into additive ones to treat them in the frequency domain using linear filters. The luminance-reflection image formation model was assumed that defines each pixel in an image as the product of the scene luminance and object reflectance within it:

$$I(x,y) = L(x,y) * R(x,y) \tag{1}$$

where L is the luminance component and R is the reflection component [33]. Ideally, the luminance component is uniform whereas reflection varies abruptly. However, lighting is not constant in a UI and these variations can be modelled as low-frequency additive noise by transforming the images into the logarithmic domain:

$$\ln(I(x,y)) = \ln(L(x,y) * R(x,y)) \tag{2}$$

$$\ln(I(x,y)) = \ln(L(x,y) + \ln(R(x,y))) \tag{3}$$

The image is transformed into the frequency domain by applying a Fourier transform and filter, *H*, which is a high pass Butterworth filter for attenuating low-frequency components. After removing low-frequency multiplicative components, an inverse Fourier transform and exponential function to return to the original image domain are applied. Figure 3 shows this sequence of steps.

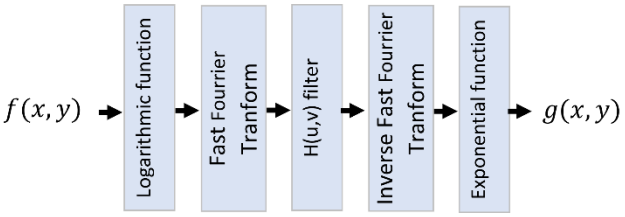

Fig. 3. Homomorphic filtering steps [32].

The CLAHE approach is a contrast enhancement technique based on balancing the cumulative density function (CDF). This was achieved by using a mapping table that allows the assignment of a more balanced apparition likeliness to every intensity value [35]. The algorithm calculates mapping values, g, for each original image intensity value, *f,* as defined in (5). In this operation, $f_{\max}$ and $f_{\min}$ are the maximum and minimum intensity values in the original image, *f,* respectively, and $P(f)$ is the uniform probability density distribution (4).

$$P(f) = \sum_{x=0}^{f} p(x) \tag{4}$$

$$G(f) = f_{\min} + P(f) * [f_{\max} - f_{\min}] \tag{5}$$

The CLAHE technique combines two techniques to avoid noise amplification and incorrect colour mapping, namely adaptive histogram equalization (AHE) and contrast limited histogram equalization (CLHE). The AHE step divides images into sectors, or neighbourhoods, to increase contrast locally [36] and CLHE establishes a parameter for limiting the contrast increase by removing pixels from the highest histogram peaks and redistributing them uniformly [37]. The CLAHE technique also permits the definition of a

preferred probability density distribution, such as the exponential and Rayleigh distributions [38] [39].

The CLAHE technique was implemented in a combined RGB-HSV colour space for restoring the colour of the fish and to make them stand out from the background. A version of the image was generated by running CLAHE on the three channels of the RGB colour space. Another version was generated by running the algorithm on the hue and saturation channels of the HSV colour space. The two enhanced images are then combined in the RGB colour space with a pixel by pixel norm as:

$$(r,g,b)=\left(\sqrt{r_1^2+r_2^2},\sqrt{g_1^2+g_2^2},\sqrt{b_1^2+b_2^2}\right) \quad (6)$$

The final part of the proposed procedure involves applying the guided filter. This method considers the input image and the content of a guidance image that can be the input image as well. This filter performs edge-preserving smoothing like the bilateral filer. However, the convolutions the guided filter performs are separable. This allows for $O(N)$ time complexity implementations independently of kernel size [40]. For this work, the parameter kernel size was set at *k=5* and regularization *eps=30*.

Two basic metrics exist for accuracy estimation of image enhancement methods, namely the mean square error (MSE) [31][41] and signal-to-noise ratio (SNR) [41]. Both metrics require a degraded image and a target image to error estimation. When no such images exist, border detection performance and histogram analysis can be used [42].

C. Segmentation techniques

Segmentation simplifies the comprehension of an image composed of thousands of pixels into a few regions [43]. The regions represent the elements that make up the image. The objects of interest are distinguished from the background based on specific local features [44].

The fish image segmentation methods were divided into four classes:

- Methods based on image histograms.
- Methods based on borders, gradients and morphological operations.
- Methods based on neighbourhoods, proximity and homogeneity
- Methods based on saliency.

Table 2 details the most relevant underwater image segmentation methods in the literature.

Histograms based Methods

Typically, histogram-based segmentation consists of three steps, namely detecting the modes of the histogram, finding the valleys between the modes and applying thresholding based on the valleys. The histogram thresholding methods are popular due to their simplicity and precision. However, they are unable to segment areas with similar intensity levels that belong to different regions. Furthermore, histogram-based methods are unable to process images with almost unimodal histograms, especially when the region of interest is much smaller than the background area [43].

The thresholding methods were classified as parametric and non-parametric. When using parametric methods, it may be assumed that the grey level distribution of each region follows a Gaussian distribution. One can then attempt to estimate the parameters to fit the histogram [45]. On the other side, non-parametric approaches find thresholds for optimally separating regions of an image based on discrimination. These approaches include inter- or intra-class variance and maximum entropy thresholds [46].

This type of segmentation was employed when working with images where the object of interest stood out from the background. When such situations occurred, images were segmented into two regions using the thresholding operator with parameter, t. This threshold value was selected by analysing the histogram [44].

Methods based on borders, gradients and morphological operations

Object border information is crucial for image processing architectures. Such information can be used for identifying and localizing sharp discontinuities that result from abrupt changes in pixel intensity [47] [48]. Methods based on borders and morphological operations simplify the image analysis by drastically reducing the amount of data other algorithms need to process [49].

Border extraction is based on detecting abrupt local changes in the intensity values of an image. The Canny border detection algorithm is among the most popular ones. It first softens the image to reduce noise and then it calculates the gradient of the image. Afterward, the algorithm detects borders based on the gradient and a threshold [50].

Morphological operations employ kernel-like structuring elements for expanding or reducing regions, to fill holes in them and to generate or remove bridges between connected areas. The morphological operations can be used to fill borders resulting from border detection algorithms.

The border-based methods are appropriate when working on images comprised of highly homogeneous regions because objects can be discriminated based on grey level changes. Otherwise, it is adequate to use neighbourhood-based segmentation algorithms [44].

Methods based on neighbourhoods and region growing

In segmentation tasks, the information provided by the environment can be exploited to obtain more homogeneous regions. This is done by exploiting statistical similarities among pixel sets belonging to the same region. The clustering by region growing starts with small seed groups. These groups grow as the algorithm finds new pixels that satisfy certain criteria [44].

There are many region-based segmentation techniques, and some of them are for general use while others are fit for specific image classes [51]. Among them, methods exist that are based on spatial feature homogeneity, whereas others focus on determining limits through discontinuity measures. Both exploit two differing definitions of “region”. Ideally, they should produce identical results, since homogeneity is the feature of a region, whereas inhomogeneity is the feature of the limit of a region [51].

Methods based on saliency

Saliency is the measure of the local contrast of elements in images with respect to their surroundings. Here, saliency was treated as a feature of the regions within an image. However, the way it was calculated is vastly different. Saliency detection algorithms typically generate maps for measuring contrast according to one or more features, such as intensity, texture and orientation. High complexity cases require generating one saliency map for every measured feature. However, a single saliency map suffices for simpler cases.

Saliency maps can be provided as input for other algorithms. Salient areas in an image are useful as seeds for region-growing techniques and remove the need for human intervention. They're also useful when carrying out border-based segmentation, as they can be used for obtaining the borders of the object of interest and as the basis for morphological operations.

Saliency detection techniques are simple but their usefulness is limited when trying to segment highly cluttered images. However, they are highly effective for segmenting underwater images captured in controlled environments where the background and foreground are clearly defined. Using the literature review as a reference, two algorithms were tested separately and a new algorithm was proposed that combines some of their features with a saliency-based approach.

Literature method 1

The method proposed by Costa *et al.* [19] was tested. This technique smooths images with a trimmed convolutional kernel of size that is *5x5*. After matching the kernel to a pixel and its neighbourhood, the authors sorted the window values and trimmed the three highest and lowest values before convoluting the central pixel. They then applied the border detection through Sobel's edge detection algorithm, a convolution method that consists of applying two kernels of uneven size: one vertically and the other horizontally. This way, they calculated the image's intensity gradient for each point and showed how abrupt the intensity changes were and the likelihood of a border existing there [52].

TABLE 2. A LITERATURE REVIEW OF SEGMENTATION TECHNIQUES

Author	Approach	Characteristics
(Canny, 1986)	Finding borders in images through derivatives and other mathematical operations.	+Canny employs mathematical equations to define two important criteria for detecting borders. +Canny shows how border detection simplifies the amount of data to be processed. -The algorithm fails with some images and generates incomplete borders.
(Freeman, 1990)	Finding borders in images using convolution kernels.	+Authors make effective use of 3x3 and 5x5 kernels for detecting borders. +They show the effectiveness of mathematically derived kernels.
(Hojjatoleslami *et al.*, 1998)	Finding borders in images through region growing.	+The region-growing method is predictable: at every step, at most one pixel fulfils the condition required to be included within a given region. +The method is efficient method for segmenting bright areas from an image with dark sections. -The implementation is less useful for processing images where the objects of interest do not stand out from the background.
(Costa *et al.*, 2006)	Extracting fish using filtering methods on stereo images.	+Authors use several techniques to filter and segment fish in images, including the *Sobel* filter. They then use morphological operations for filling borders and obtaining the whole fish region. -If the images are too complex or if the fishes are distorted, segmentation produces bad results.
(Mitianoudis *et al.*, 2008)	Image fusion using pixel or region-based rules.	+The authors carry out image fusion by modifying the main channels of the image.
(Yao *et al.*, 2013)	Improved K-means method for image segmentation.	+Authors define the number of clusters required to segment an image as a function of its histogram. -If the number of clusters is too big, the algorithm can over-segment the image, and time complexity grows. If it is too small, it segments the objective region incompletely.
(Zhang *et al.*, 2014)	Combination of dependent thresholding and Sobel's segmentation method.	+The method the authors propose has satisfactory results for brain tumor candidate border detection. +The method generates closed contours when the conditions are adequate. -The method fails to segment images properly where borders are not sufficiently marked.
(Wang *et al.*, 2016)	Authors propose segmenting color images based on pixel classification using quaternion exponent moments.	+Authors extract pixelwise features from images based on quaternion exponent moments. They determine pixel content by considering correlation among different color channels. +Authors execute computational operations more quickly and efficiently by using a classifier.
(Ben *et al.*, 2017)	Authors present a multilevel extension of the multidimensional thresholding method for gray image segmentation.	+The two-dimensional threshold results in effective segmentation when images suffer from noise, shading or reflection effects. -Computational cost is high, and thresholding must be parametrized.
(Oiao *et al.*, 2017)	Image segmentation using an active contour method.	+Authors decompose images into their primary channels to carry out image fusion for segmentation purposes. -Parts of the background such as ground sedimentation can have a negative effect on segmentation as they blend with the object of interest.

+ Strength
- Weakness

Both masks used by the algorithm are defined in (7), where Δx and Δy are the horizontal and vertical masks, respectively:

$$\Delta x = \begin{bmatrix} -1 & 0 & 1 \\ -2 & 0 & 2 \\ -1 & 0 & 1 \end{bmatrix} \quad \Delta y = \begin{bmatrix} 1 & 2 & 1 \\ 0 & 0 & 0 \\ -1 & -2 & -1 \end{bmatrix} \tag{7}$$

We use simple thresholding with a fixed grey threshold level of 24 that they defined empirically. To enhance the contours generated by previous steps and to make them less fragmented, they processed each image once more by using a set of morphological operations, namely erosion, dilation, closing and opening.

Erosion removes small details in an image, such as noise, but also reduces the region of interest's size. Dilation of an image, f, through a structuring element, s($f \oplus s$), produces a new binary image, $g = f \oplus s$. It places them in all *(x, y)* coordinates where the structuring element intersects with the input image, f. In other words, *g (x, y) = 1* if any part of *s* hits an area within *f* already equal to 1, and it is 0 otherwise. This is repeated for every pixel coordinate *(x, y)*. Dilation is the opposite of erosion because it adds a layer of pixels to external and internal region limits [57].

After dilation, the authors employed the closing operation. Closing an *f* image with a structuring element, $s(f \bullet s)$, entails carrying out dilation immediately followed by erosion, where $f \bullet s = (f \oplus s) \ominus s$. Closing gets its name from the fact it can close holes in regions of the image while they maintain their original sizes.

Lastly, authors applied an opening filter. The opening of an image, ***f***, is the result of using a structuring element, ***s*** (defined as $f \circ s$), and applying the erosion filter followed by the dilation filter to restore regions surviving erosion to their original size. Thus, $f \circ s = (f \ominus s) \oplus s$ [57]. Opening is the dual operation of closing:

$$f \bullet s = (f^c \circ s)^c; \quad f \circ s = (f^c \bullet s)^c \tag{8}$$

This method is useful due to the pre-processing the authors carried out before border detection. However, choosing a fixed thresholding value sometimes results in under- or over-segmentation of areas of the fish.

Literature method 2

Yao *et al.* [54] developed an improved version of the K-means clustering algorithm for segmenting fish images. The first step is to smoothen the grey level histogram. Afterward, they selected a *K* value by counting the most relevant peaks while accounting for a distance criterion. The average distance between peaks, *p*, is the sum of the distances between each successive couple of histogram peaks and valleys, defined as *i* and divided by the number of peak/valley pairs *M* (9). If the distance between the two peaks in the histogram is less than the average distance, they discard the smaller peak to guarantee the algorithm only counts the most relevant peaks:

$$p = \frac{1}{M} \sum_{i=0}^{M} dis(i) \tag{9}$$

The next step is finding the initial values for the K-means clusters. The Otsu method consists of finding a threshold to minimize intra-class variance among pixels classified as black, σ_0^2, and those classified as white, σ_1^2, as shown in Equation (10).

$$\sigma_w^2 = w_0(t)\sigma_0^2(t) + w_1(t)\sigma_1^2(t) \tag{10}$$

After the threshold calculation, the method calculates *K* initial cluster centres and the median value, *m*. It compares this value with the threshold, *t*, resulting from executing Otsu. If the difference between values is less than the average distance between histogram peaks, *p*, the starting values are used for the K-means algorithm. Otherwise, the algorithm randomly samples another set of *K* centres.

The K-means clustering method consists of minimizing a *J* value, given *N* individuals and *K* starting centres. When a value, *n*, is not within cluster, *k*, the γ value will be 0. Otherwise, its value is 1 and allows the distances between values and their respective centres to be quantified, as shown in Equation (11):

$$J = \sum_{n=1}^{N} \sum_{k=1}^{K} \|x_n - \mu_k\|^2 \mathrm{Y}_{nk} \tag{11}$$

After clustering, two or more grey levels are present in the image, but noise and small holes may remain. The authors employed morphology techniques to address this issue. Specifically, they used morphological closing and opening operations, in addition to hole filling, for obtaining the final fish silhouette. The authors managed to improve over traditional methods, although they did not test their proposal on actual underwater images.

Proposed method

Both [19] and [54] generate an incomplete fish silhouette and fill it with morphological operations. This study raises the possibility of combining a more appropriate saliency-based method with the morphological approaches these authors describe.

First, the pre-processed image is taken and the mean of every colour channel is calculated, as described in Equation (12):

$$C_m = mean(I_C) \tag{12}$$

where *I* is the original image, *C* is the selected channel and C_m is its mean. Once the mean is calculated for each channel, the square of the difference between it and the channel's mean is assigned to each pixel. The resulting image, *S*, corresponds to the intensity of the pixel values with respect to the whole channel, as shown in Equation (13):

$$S(x,y,c) = (I(x,y,c) - C_m)^2 \tag{13}$$

After calculating S, it is transformed into a grey-scale image. Next, the Sobel filter is used in the same way as [19] for generating borders from the saliency map. A fixed threshold of *t=3* was defined to maintain fish edges only

and remove borders corresponding to noise and background intensity variations. Any remaining noise is removed by deleting connected components whose area is less than 50 pixels.

Three iterations of erosion, dilation, opening and closing are applied and followed by a hole filling operation. An elliptical structuring element is used (see Fig. 5) for fitting the shape of the fish instead of a generic one. Also, since the possibility of background noise may remain from the previous steps, the biggest non-black connected component is selected and any other elements from the resulting image are removed.

D. Determining the best line to measure the fish orientation

The aim of this work is the automation of the fish measurement process through computational techniques. Several studies show that a strong correlation exists between weight and length for more than 50 different species of fish [58]–[62]. This makes length measurement appropriate for estimating fish weight, and motivates our decision to make length measurement as part of the pipeline. In our setup, the fish is assumed to be positioned along the x-axis since it does not allow for high variations in fish orientation. For calculating fish length, a line that adheres to the following criteria must be found:

a. It goes from the nose of the fish to the fork of its tail.
b. It is not excessively affected by the fins of the fish.
c. It can adapt to the fish's flexible nature.

Figure 6 shows the most relevant measurements for estimating fish length. W_4 represents the actual length of the fish, while W_1 to W_3 correspond to the vertical section lengths of the fish from head to tail. Using the mid-points of each W, it is possible to estimate W_4. The line that best represents fish length should connect the midpoints of the fish along the longest axis to satisfy condition (c). Afterward, regression can be applied and the length in pixels of the resulting line or curve can be calculated. Conditions (b) and (c) can be satisfied by using polynomial regression methods.

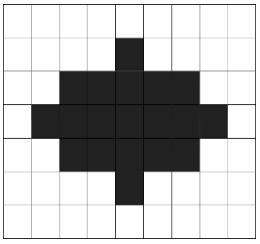

Fig. 5. Structuring element of 5x7 pixels.

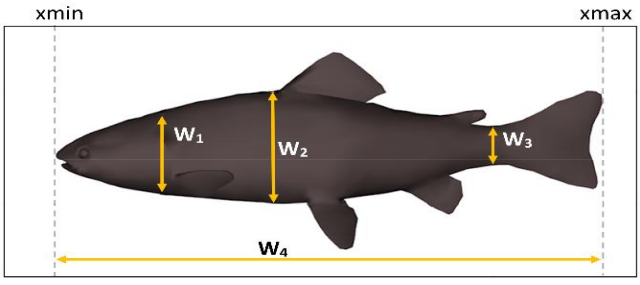

Fig. 6. Methodology for determining fish mid-points.

III. RESULT AND DISCUSSION

A. Proposed Imaging System

A system based on that of Zion *et al.* [21] is proposed in this work (see Fig. 7(a)). For this system, the pond is divided into two sections with a grid and they are connected with a pair of parallel tunnels with unidirectional doors. A sealed compartment is attached to the side of one of the tunnels, which is separated by a glass wall. A camera is placed in the compartment and connected to a computer for capturing the fish images.

a)

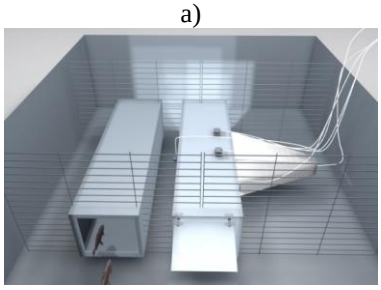

b)

Fig. 7. Internal view of the proposed system.

To facilitate image processing, five lights in the main tunnel are set up in the main tunnel. Four of them are around the window between the tunnel and the container and one is in the tunnel wall directly in front of the camera, as shown in Figures 7(b) and (c). This allows backlighting of the fish and a sharper side-view.

B. Image Processing and Segmentation

Table 3 shows the results of applying the literature segmentation methods as well as two versions of this pipeline (testing bilateral and guided filters) on a subset of 30 images extracted from the QUT (Queensland University of Technology) dataset [58] and other similar databases [59]– [64]. The images were resized to 450x700 and pre-processed with the homomorphic Filter CLAHE RGBHSV-guided filter sequence before running out the segmentation algorithm. Figure 8 shows the results of the complete sequence.

A segmented pixel is segmented correctly if it is labelled as part of the fish in the manually segmented version of the image and it is labelled the same by the algorithm. The amount of over-segmentation is measured based on the number of pixels wrongly marked as part of the fish and the total amount of pixels we manually labelled as part of the fish. Under segmentation is calculated based on pixels belonging to the fish the algorithms segmented as part of the background, as well as the total amount of fish pixels in the ground truth.

Figure 9 depicts the results from this study, black and white sections represent parts of the image the algorithms labelled correctly, while red areas represent under segmented or over segmented parts of the image. As

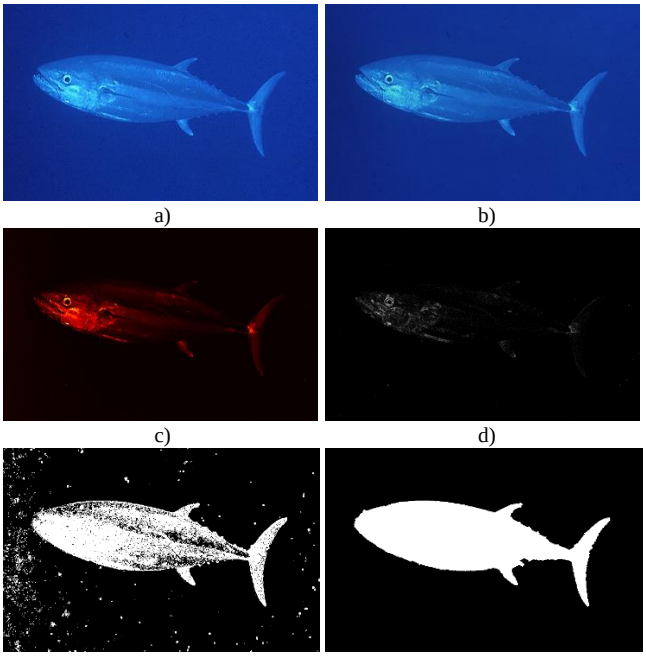

Fig. 8. a) Original image, b) pre-processed image, c) saliency map, d) edge detection with the Sobel filter, e) image after thresholding and f) final segmented image after morphological operations.

observed in Table 3, this segmentation method had a correct classification rate slightly superior to that of [19] and well above [54] when using a guided filter as part of the pre-processing sequence. However, results were not remarkable when employing the bilateral filter.

The guided filter-based version of this algorithm resulted in more over segmentation when compared to the method of Costa *et al*. However, it had the least under-segmentation of all four implementations and is the algorithm that best preserved the shape of the fish. The algorithm proposed by Yao *et al.* resulted in considerable over-segmentation when compared to the other methods. Although the bilateral filter version of our method results in the least rate of under-segmentation, it came at the cost of excessive over-segmentation.

Concerning execution times, the fastest method was the proposed saliency-based segmentation with a guided-filter as part of the pre-processing step. It averaged 1.26 seconds for every 450x700 image processed. This was followed by the bilateral-filter version of the same algorithm with 1.56 seconds. The increase was due to the higher computational complexity of the bilateral filter. Next came the algorithms of Yao *et al.* and Costa *et al.* with 2.75 and 3.30 seconds, respectively. Both algorithms were held back by their most expensive segments: computing the K-means algorithm and the (non-separable) trimmed kernel convolution.

C. Fish Measurement

The mid-points of the fish were generated as described in Section 2.4 and are the target values for several regression methods: linear regression, grade 3 polynomial regression, grade 4 polynomial regressions, k-nearest neighbours and support vector regression. In the case of polynomial regression, this results in a line curve, *f*, which fits the length of the fish, as shown in Equation 14, where *a*, *b*, *c* and *d* are the polynomial parameters:

$$f(x) = ax^3 + bx^2 + cx + d \tag{14}$$

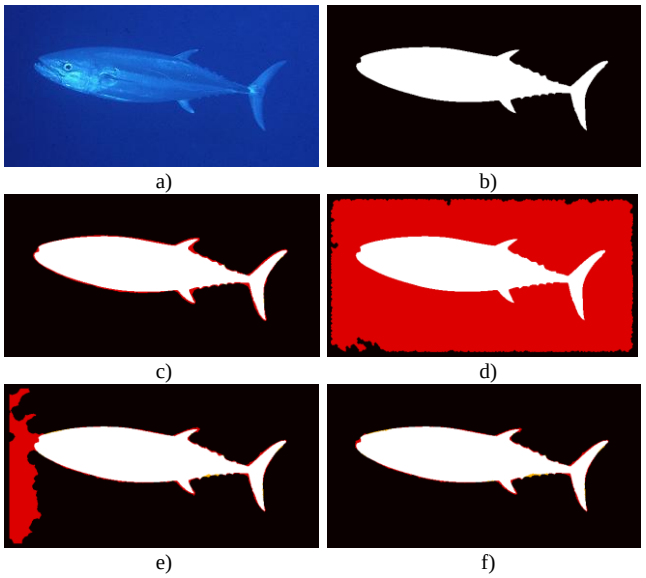

Fig. 9. Application of segmentation methods shown in Table 3: a) original image, b) ground truth, c) image segmented by [19], d) image segmented by [54], e) proposed method with bilateral filter and f) proposed method with guided filter.

Calculating arc length for polynomials using integration is a non-trivial task, so the arc length is calculated by evaluating *x* values between $x_{\min}$ and $x_{\max}$ with step 1. The distance $d(x_i, x_{i+1})$ is calculated and added between each pair of successive *x* values to obtain the total length, *s*.

The length and weight of 150 fish specimens of *Orechromis niloticus* belonging to the *Cichlidae* family were registered in this manner, and used for testing the proposed methodology. Photos were taken on a table with a reference square of 4x4 cm. Their manual segmentations were also generated. Once the fish length, *s*, was calculated in pixels in the manually segmented image, *s* was converted to centimetres by using the square as a reference.

TABLE 3. THE EVALUATION OF SEGMENTATION METHODS.

Method	Correctly Segmented (Average)	Incorrectly Segmented (Average)	Over segmented (Average)	Under segmented (Average)	Time per Image (Average)
(Costa *et al*., 2006)	86.8%	13.2%	4.97%	7.11%	3.30 seconds
(Yao *et al*., 2013)	75.85%	24.25%	68.34%	2.11%	2.75 seconds
Proposed method (bilateral filter)	82.69%	17.31%	26.80%	0.96%	1.56 seconds
Proposed method (guided filter)	87.94%	12.04%	6.07%	1.49%	1.26 seconds

The manual segmentation images were used as the ground truth set in segmentation accuracy measurement. As the weights of fishes were known, several regression algorithms were run on half of said data for training an estimator for the weight of new fishes. The tested regression methods for weight estimation were single variable linear regression, grade 3 polynomial regression, grade 4 polynomial regression, k-nearest neighbours and support vector regression.

TABLE 4. ERROR ESTIMATION FOR REGRESSION OF REAL FISH LENGTH.

	RMSE	MAE	MAPE	MSLE	EVS	R^2
Lineal	1.5142	1.1821	4.9077	0.0034	0.9446	0.9382
Polynomial^3	1.1479	0.8879	3.6323	0.0022	0.9794	0.9602
Polynomial^4	1.2112	0.9531	3.7980	0.0023	0.9800	0.9578
k-NN	2.6790	2.4491	9.1401	0.0098	0.9691	0.8123
SVR	5.9643	4.1413	13.0482	0.0387	0.6290	0.4471

Figure 10 shows five examples of the curve estimation for length measurement from segmented images. Subfigures on the left side correspond to original segmented images by the proposed method with the guided filter. Subfigures on the right side show the estimated curve used for length estimation using a pixels-centimetres relation. The length and weight of the fishes on the Fig. 10, are listed in Table 7.

Table 4 shows the length estimation error for the five regression methods on the half the tabulated data. Six metrics were employed: root of the mean squared error (RMSE), mean absolute error (MAE), mean absolute percentage error (MAPE), mean square logarithmic error (MSLE), explained variance score (EVS) and the R^2 score metric. Figure 11 depicts the ground-truth results and the graphical behaviour of the six methods when run on the testing set.

TABLE 5. ERROR ESTIMATION FOR REGRESSION OF TEST SET FISH WEIGHT BASED ON REAL FISH LENGTH.

	RMSE	MAE	MAPE	MSLE	EVS	R^2
Lineal	0.0512	0.0341	53.4839	0.0016	0. 8324	0.8324
Polynomial^3	0.0238	0.0113	12.8840	0.0004	0.9637	0.9637
Polynomial^4	0.0235	0.0113	14.1317	0.0004	0.9646	0.9646
k-NN	0.0341	0.0134	11.7580	0.0005	0.9256	0.9254
SVR	0.0939	0.0530	69.1921	0.0040	0.4393	0.4351

TABLE 6. ERROR ESTIMATION FOR REGRESSION OF TEST SET FISH WEIGHT BASED ON ESTIMATED FISH LENGTH.

	RMSE	MAE	MAPE	MSLE	EVS	R^2
Lineal	0.0797	0.0572	28.0965	0.0029	0.8303	0.8254
Polynomial^3	0.0309	0.0244	11.2469	0.0004	0.9772	0.9736
Polynomial^4	0.0323	0.0253	11.8869	0.0005	0.9758	0.9713
k-NN	0.0694	0.0402	13.2213	0.0020	0.8765	0.8676
SVR	0.2133	0.1503	48.6063	0.0157	0.3383	-0.250

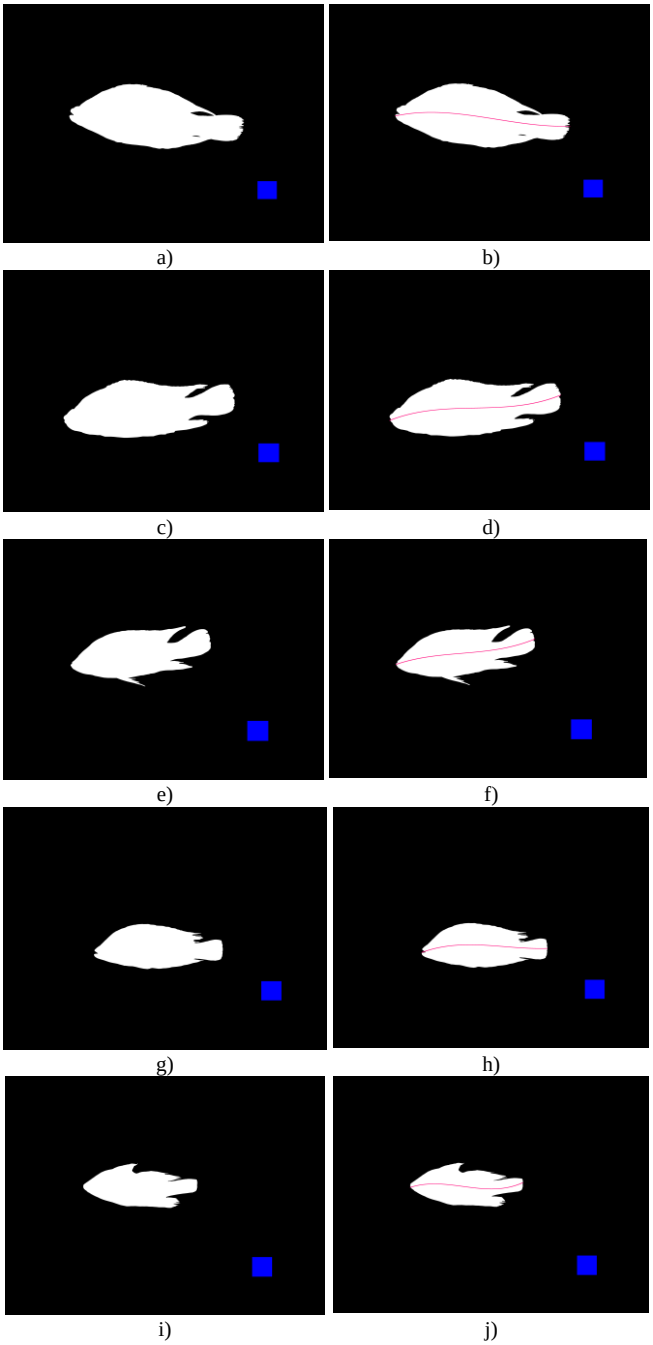

Fig. 10. Examples of measurement algorithm application to test set: a,c,e, g, i) segmented images, b,d,f, h, j) estimated curve for length measurement. The blue square was used to establish the pixels-centimeters relation.

Table 5 depicts the results of weight estimation of the other 75 fish, based on real fish length. Table 6 displays the results of weight regression based on estimated fish length, for the same fishes.

As seen in Table 4 to 6 and Figure 11, the best results for all cases were obtained when using grade 3 polynomial regression for estimating fish length and fish weight. Grade 4 polynomial regression was almost as efficient, while k-NN was somewhat worse than both polynomial algorithms. In contrast, methods such as linear regression and SVR were not as precise.

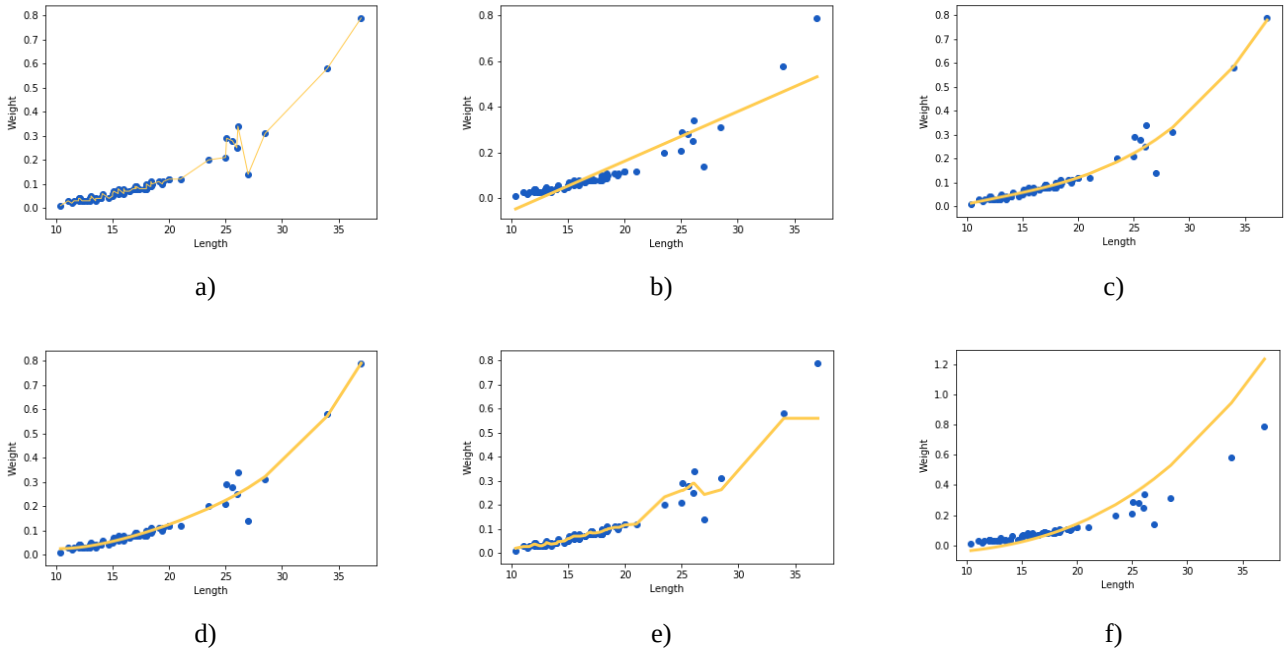

Fig. 11. Graphical behaviour of regression of real fish weight-length relationship: a) real data, b) lineal regression, c) grade 3 polynomial regression, d) grade 4 polynomial regressions, e) k-NN regression and f) support vector regression.

IV. Conclusions

Problems such as lighting inequalities, poor contrast and noise are obstacles to the implementation of computer vision technologies. Although extensive research has been carried out to deal with these problems, it is often difficult to apply solutions intended for non-subaquatic contexts for segmentation tasks in underwater environments.

In this case, the requirement of segmenting fishes before measurement made it necessary to work with images where these issues were managed, which is hard to accomplish in uncontrolled settings.

The proposed approach of a single camera imaging system in a controlled environment was expected to improve image capture conditions, as backlighting techniques and an enclosed environment help to reduce external lightning and sedimentation to acceptable levels. The proposed system makes use of a mechanism for forcing fish to transit through unidirectional tunnels separating the hatchery. By exploiting feeding schedules, their movement will be controlled, guaranteeing the representativeness of the sample.

Table 7. Examples of length and weight estimation.

	Length(cm)		Weight (gr)	
Subfigure	Real	Estimated	Real	Estimated
a	37.12	37.701	791	7801
c	34.05	35.197	580	586.1
e	28.50	28.710	310	330.3
g	25.11	26.467	290	224.6
i	23.50	24.045	201	185.8

After obtaining the images, it was necessary to enhance them. The image pre-processing proposed in [29] was made more helpful toward segmentation and faster to execute by combining homomorphic filtering for lighting balance, CLAHE for contrast enhancement and guided filtering for noise reduction and border highlighting. The use of CLAHE in combined HSV-RGB colour space gave particularly good results when executed on the dataset. The proposed segmentation pipeline combined the morphological principles of [19] and [54] with a relatively simple 2D saliency detection method. The proposed algorithm showed remarkable effectiveness when carrying out fish segmentation.

As for fish measurement and weighing, the fish was assumed to be positioned along the x-axis given the proposed setup. Results showed that relatively simple methods, such as polynomial regression, can be employed for calculating the fish length and estimating its weight with remarkable accuracy. Grade-3 polynomial regression resulted in an error of less than 4% for length estimation, while grade-3 and grade-4 polynomial regressions resulted in errors of 11.24% and 11.88% respectively for fish weight estimation. This means the methods will allow precise estimation of fish weight and adequate calculation of the food needs of hatcheries.

References

[1] AUNAP, «La pesca y la acuicultura en Colombia», Autoridad nacional de acuicultura y pesca - AUNAP., Bogotá D.C., may 2014.

[2] AUNAP, «Plan nacional para el desarrollo de la acuicultura sostenible en Colombia - PlanDAS», Autoridad nacional de acuicultura y pesca - AUNAP., Bogotá D.C., feb. 2014.

[3] Ministerio de Agricultura, «Decreto 4181 de 2011, por medio del cual se escindieron unas funciones del INCODER y del Ministerio de Agricultura y Desarrollo Rural, y creó la Autoridad Nacional de acuicultura y pesca – AUNAP» 2011.

[4] J. M. Ecoutin, J. J. Albaret, y S. Trape, «Length–weight relationships for fish populations of a relatively undisturbed tropical estuary: The Gambia», Fish. Res., vol. 72, n.o 2, pp. 347-351, may 2005.

[5] C. Niyonkuru y P. Laleye, «A Comparative Ecological Approach of the Length–Weight Relationships and Condition Factor of Sarotherodon Melanotheron Rüppell, 1852 and Tilapia Guineensis

(Bleeker 1862) in Lakes Nokoué and Ahémé (Bénin, West Africa)», Int. J. Bus. Humanit. Technol., vol. 2, n.o 3, pp. 41–50, 2012.
[6] B. Zion, A. Shklyar, y I. Karplus, «Sorting fish by computer vision», Comput. Electron. Agric., vol. 23, n.o 3, pp. 175-187, sep. 1999.
[7] C. Turan, M. Oral, B. Öztürk, y E. Düzgüneş, «Morphometric and meristic variation between stocks of Bluefish (Pomatomus saltatrix) in the Black, Marmara, Aegean and northeastern Mediterranean Seas», Fish. Res., vol. 79, n.o 1, pp. 139-147, jun. 2006.
[8] J. Ovredal and B. Totland, «The scantrol fish meter for recording fish length, weight and biological data», Fish. Res., vol. 55, pp. 325-328, 2002.
[9] M. Li y X. Zhang, «Theoretical Analysis on Automatization and Human-Machine Combination», Intell. Hum-Mach. Syst. Cybern. 2009, vol. 1, pp. 417-422, ago. 2009.
[10] R. W. Hardin, «Vision system monitors fish populations», Vision Systems Design, vol. 11, n.o 1, pp. 41,43-45, 2006.
[11] B. Zion, «The use of computer vision technologies in aquaculture – A review», Comput. Electron. Agric., vol. 88, pp. 125-132, oct. 2012.
[12] N. J. C. Strachan, «Length measurement of fish by computer vision», Comput. Electron. Agric., vol. 8, n.o 2, pp. 93–104, 1993.
[13] R. J. Petrell, X. Shi, R. K. Ward, A. Naiberg, y C. R. Savage, «Determining fish size and swimming speed in cages and tanks using simple video techniques», Aquac. Eng., vol. 16, n.o 1–2, pp. 63-84, 1997.
[14] R. Tillett, N. McFarlane, y J. Lines, «Estimating dimensions of free-swimming fish using 3D point distribution models», Comput. Vis. Image Underst., vol. 79, n.o 1, pp. 123-141, 2000.
[15] J. A. Lines, R. D. Tillett, L. G. Ross, D. Chan, S. Hockaday, y N. J. B. McFarlane, «An automatic image-based system for estimating the mass of free-swimming fish», Comput. Electron. Agric., vol. 31, n.o 2, pp. 151-168, abr. 2001.
[16] M. Chambah, D. Semani, A. Renouf, P. Courtellemont, y A. Rizzi, «Underwater color constancy: enhancement of automatic live fish recognition», 2003, vol. 5293, pp. 157-168.
[17] J. R. Martinez-De Dios, C. Serna, y A. Ollero, «Computer vision and robotics techniques in fish farms», Robotica, vol. 21, n.o 3, pp. 233-243, 2003.
[18] D.-J. Lee, R. B. Schoenberger, D. Shiozawa, X. Xu, y P. Zhan, «Contour matching for a fish recognition and migration-monitoring system», 2004, p. 37.
[19] D. J. White, C. Svellingen, y N. J. C. Strachan, «Automated measurement of species and length of fish by computer vision», Fish. Res., vol. 80, n.o 2-3, pp. 203-210, 2006.
[20] C. Costa, A. Loy, S. Cataudella, D. Davis, y M. Scardi, «Extracting fish size using dual underwater cameras», Aquac. Eng., vol. 35, n.o 3, pp. 218-227, oct. 2006.
[21] K. Lam, R. S. Bradbeer, P. K. Shin, K. K. Ku, y P. Hodgson, «Application of a real-time underwater surveillance camera in monitoring of fish assemblages on shallow coral communities in a marine park», en OCEANS 2007, 2007, pp. 1–7.
[22] B. Zion, V. Alchanatis, V. Ostrovsky, A. Barki, y I. Karplus, «Real-time underwater sorting of edible fish species», Comput. Electron. Agric., vol. 56, n.o 1, pp. 34-45, mar. 2007.
[23] C. Costa, F. Antonucci, C. Boglione, P. Menesatti, M. Vandeputte, y B. Chatain, «Automated sorting for size, sex and skeletal anomalies of cultured seabass using external shape analysis», Aquac. Eng., vol. 52, pp. 58-64, ene. 2013.
[24] Z. Liu, F. Cheng, y W. Zhang, «A novel segmentation algorithm for clustered flexional agricultural products based on image analysis», Comput. Electron. Agric., vol. 126, pp. 44-54, ago. 2016.
[25] H. Qin, X. Li, J. Liang, Y. Peng, y C. Zhang, «DeepFish: Accurate underwater live fish recognition with a deep architecture», Neurocomputing, vol. 187, pp. 49-58, abr. 2016.
[26] J. M. Miranda y M. Romero, «A prototype to measure rainbow trout's length using image processing», Aquac. Eng., vol. 76, pp. 41-49, 2017.
[27] K. Iqbal, R. Abdul Salam, A. Osman, and A. Zawawi Talib, "Underwater image enhancement using an integrated color model," IAENG International Journal of Computer Science, vol. 34, no. 2, pp. 239-244, 2007.
[28] R. Wang, Y. Wang, J. Zhang, y X. Fu, «Review on underwater image restoration and enhancement algorithms», 2015, pp. 1-6.
[29] S. Serikawa y H. Lu, «Underwater image dehazing using joint trilateral filter», Comput. Electr. Eng., vol. 40, n.o 1, pp. 41-50, ene. 2014.
[30] A. Ceballos-Arroyo, I. Diaz-Bolano, y G. Sanchez-Torres, «Analyzing pre-processing filters sequences for underwater-image enhancement», Contemp. Eng. Sci., vol. 10, pp. 751-771, 2017.
[31] D. S. Baajwa, S. A. Khan, y J. Kaur, «Evaluating the Research Gaps of Underwater Image Enhancement Techniques», Int. J. Comput. Appl., vol. 117, n.o 20, 2015.
[32] B. Singh, R. S. Mishra, y P. Gour, «Analysis of contrast enhancement techniques for underwater image», Int. J. Comput. Technol. Electron. Eng., vol. 1, n.o 2, pp. 190–194, 2011.
[33] G. Hou, G. Wang, Z. Pan, B. Huang, H. Yang, and T. Yu, "Image Enhancement and Restoration: State of the Art of Variational Retinex Models," IAENG International Journal of Computer Science, vol. 44, no.4, pp445-455, 2017.
[34] «Enhancement by Point Processing», sep-2004.
[35] R. C. Gonzales y R. E. Woods, Digital Image Processing, 2nd ed. Boston, MA, USA: Addison-Wesley Longman Publishing Co., Inc., 2002.
[36] N. M. Sasi y V. K. Jayasree, «Contrast Limited Adaptive Histogram Equalization for Qualitative Enhancement of Myocardial Perfusion Images», Engineering, vol. 05, n.o 10, pp. 326-331, 2013.
[37] R. C. Austin y A. Geselowit, «Adaptive Histogram Equalization and Its Variations», 1986.
[38] G. Hajargasht, «Stochastic frontiers with a Rayleigh distribution», J. Product. Anal., vol. 44, n.o 2, pp. 199-208, oct. 2015.
[39] «Contrast-limited adaptive histogram equalization (CLAHE) - MATLAB adapthisteq», 2006.
[40] K. He, J. Sun, y X. Tang, «Guided Image Filtering BT - link.springer.com», Link.Springer.Com, vol. 6311, n.o Chapter 1, pp. 1-14, 2010.
[41] G. Padmavathi, P. Subashini, M. M. Kumar, y S. K. Thakur, «Comparison of filters used for underwater image pre-processing», IJCSNS, vol. 10, n.o 1, pp. 58–65, 2010.
[42] K. Iqbal, M. Odetayo, y A. James, «Enhancing the low-quality images using Unsupervised Colour Correction Method», 2010, pp. 1703-1709.
[43] X.-Y. Wang, Z.-F. Wu, L. Chen, H.-L. Zheng, y H.-Y. Yang, «Pixel classification based color image segmentation using quaternion exponent moments», Neural Netw. Off. J. Int. Neural Netw. Soc., vol. 74, pp. 1-13, feb. 2016.
[44] J. Muñóz Pérez, «Procesamiento Digital de Imágenes», Página personal de José Muñoz Pérez, 2010.
[45] A. Ben Ishak, «A two-dimensional multilevel thresholding method for image segmentation», Appl. Soft Comput. J., vol. 52, pp. 306-322, mar. 2017.
[46] J. Zhang, H. Li, Z. Tang, Q. Lu, X. Zheng, y J. Zhou, «An Improved Quantum-Inspired Genetic Algorithm for Image Multilevel Thresholding Segmentation», Math. Probl. Eng., vol. 2014, pp. 1-12, 2014.
[47] H. Du, M. Li, y J. Meng, «Study of fluid edge detection and tracking method in glass flume based on image processing technology», Adv. Eng. Softw., may 2017.
[48] Y. Ryu, Y. Park, J. Kim, and S. Lee, "Image Edge Detection using Fuzzy C-means and Three Directions Image Shift Method," IAENG International Journal of Computer Science, vol. 45, no.1, pp1-6, 2018.
[49] J. Canny, «A computational approach to edge detection», IEEE Trans. Pattern Anal. Mach. Intell., n.o 6, pp. 679–698, 1986.
[50] A. Aslam, E. Khan, y M. M. S. Beg, «Improved Edge Detection Algorithm for Brain Tumor Segmentation», Procedia Comput. Sci., vol. 58, pp. 430-437, 2015.
[51] S. A. Hojjatoleslami y J. Kittler, «Region growing: a new approach», IEEE Trans. Image Process., vol. 7, n.o 7, pp. 1079-1084, jul. 1998.
[52] H. Freeman, Ed., Machine vision for three-dimensional scenes: [annual workshop, held in New Brunswick, April 1989]. Boston: Academic Press, 1990.
[53] N. Mitianoudis y T. Stathaki, «Image fusion schemes using ICA bases», Image Fusion Algorithms Appl., p. 85, 2008.
[54] H. Yao, Q. Duan, D. Li, y J. Wang, «An improved k-means clustering algorithm for fish image segmentation», Math. Comput. Model., vol. 58, n.o 3–4, pp. 790-798, 2012.
[55] X. Qiao, J. Bao, L. Zeng, J. Zou, y D. Li, «An automatic active contour method for sea cucumber segmentation in natural underwater environments», Comput. Electron. Agric., vol. 135, pp. 134-142, abr. 2017.
[56] D. Ray, «Edge Detection in Digital Image Processing», Univ. Wash. Dep. Math., 2013.
[57] M. J. B. Wilhelm Burger, Digital Image Processing: A Practical Introduction Using JavaTM, 1.a ed., vol. 1. Pearson Education, 2000.

[58] K. Anantharajah et al., «Local inter-session variability modelling for object classification», en 2014 IEEE Winter Conference on Applications of Computer Vision (WACV), 2014, pp. 309-316.
[59] C. Ancuti, C. O. Ancuti, T. Haber, y P. Bekaert, «Enhancing underwater images and videos by fusion», en 2012 IEEE Conference on Computer Vision and Pattern Recognition (CVPR), 2012, pp. 81-88.
[60] N. Carlevaris-Bianco, A. Mohan, y R. M. Eustice, «Initial results in underwater single image dehazing», 2010, pp. 1-8.
[61] S. Emberton, L. Chittka, y A. Cavallaro, «Hierarchical rank-based veiling light estimation for underwater dehazing», 2015, pp. 125.1-125.12.
[62] R. Fattal, «Single image dehazing», ACM Trans. Graph. TOG, vol. 27, n.o 3, p. 72, 2008.
[63] A. Galdran, D. Pardo, A. Picón, y A. Alvarez-Gila, «Automatic Red-Channel underwater image restoration», J. Vis. Commun. Image Represent., vol. 26, pp. 132-145, 2015.
[64] H. Lu, Y. Li, L. Zhang, y S. Serikawa, «Contrast enhancement for images in turbid water», J. Opt. Soc. Am. A Opt. Image Sci. Vis., vol. 32, n.o 5, pp. 886-893, 2015.